

S. Calatroni, F. Gerigk, W. Weingarten

SC cavities: performance as a function of frequency and temperature

Outline

- Choice of accelerating gradient
 - Remarks concerning $\beta < 1$ cavities
 - Simulation of $Q(E_a)$
 - Deterministic parameters
 - Stochastic parameters
 - Look towards other laboratories
 - CERN (1985)
 - DESY
 - ORNL/JLAB
- Choice of operating temperature T_b and frequency ω
 - Power grid – beam transfer efficiency (T_b, ω)
 - Remarks concerning cryostat
- Concluding remarks

Choice of accelerating gradient

Remarks concerning $\beta < 1$ cavities

TM waves in waveguides of arbitrary cross section

Electromagnetic waves guided along a uniform system in z direction

Transverse magnetic waves

Cylindrical symmetry

$$\left. \begin{aligned} \nabla^2 \vec{E} &= -k^2 \vec{E} \\ \nabla^2 &= \nabla_{xy}^2 + \frac{\partial^2}{\partial z^2} \\ \frac{\partial^2}{\partial z^2} &= \gamma^2 \end{aligned} \right\} \Rightarrow \nabla_{xy}^2 \vec{E} = -(\underbrace{\gamma^2 + \overbrace{k^2}^{(\frac{\omega}{c})^2}}_{k_c^2}) \vec{E} \Rightarrow \nabla_{xy}^2 E_z = \frac{\partial^2 E_z}{\partial r^2} + \frac{1}{r} \frac{\partial E_z}{\partial r} + \frac{1}{r^2} \underbrace{\frac{\partial^2 E_z}{\partial \phi^2}}_{=0} = -k_c^2 E_z$$

Pillbox resonator with
metallic wall at $r = R$:
 $\mathbf{E}_z = \mathbf{0}$

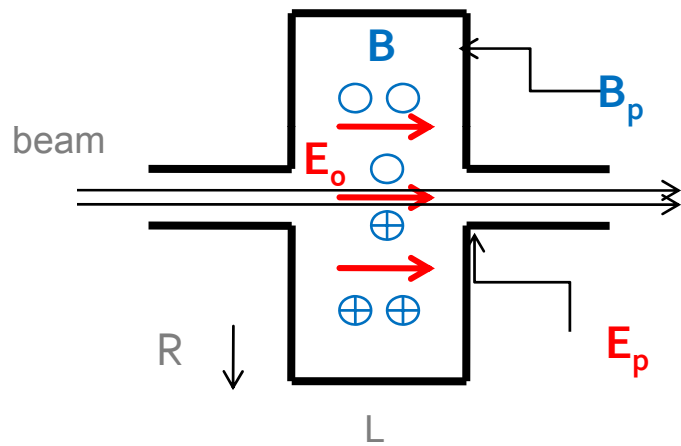
$$\gamma = 0 \Rightarrow \frac{\partial^2 E_z}{\partial r^2} + \frac{1}{r} \frac{\partial E_z}{\partial r} + \left(\frac{\omega}{c}\right)^2 E_z = 0$$

$$E_z(r) = E_0 \cdot J_0\left(\frac{\omega}{c} \cdot r\right) = E_0 \cdot J_0\left(2.405 \cdot \frac{r}{R}\right)$$

Choice of accelerating gradient
Remarks concerning $\beta < 1$ cavities

Definition of accelerating gradient

The unavoidable beam tube opening is considered to be small compared to λ



$$E(r, t) = J_0\left(\frac{2.405 \cdot r}{R}\right) \cdot E_0 \sin(\omega_0 \cdot t)$$

$$t(z) = z / (\beta \cdot c)$$

$$L = \beta \cdot \frac{\lambda}{2}$$

$$W|_{r=0} = e \int_0^L E(r=0, t(z)) dz = e E_0 \cdot \int_0^L \sin(\omega_0 \cdot z / (\beta \cdot c)) dz =$$

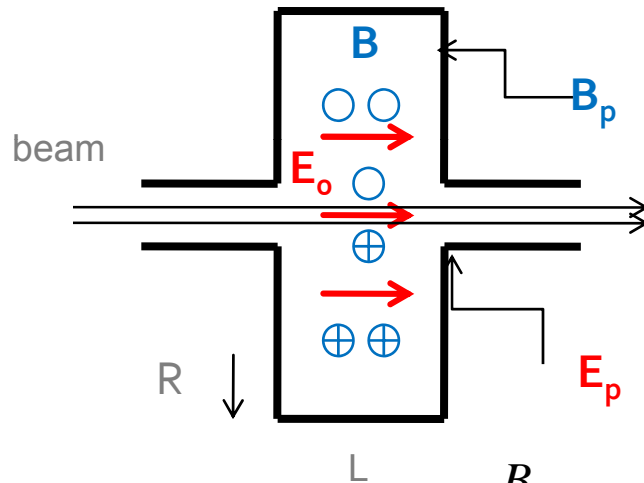
$$V_a = \frac{W}{e} = \frac{E_a \cdot L}{e} = E_0 \cdot \frac{2}{\pi} \cdot L \Rightarrow E_a = \frac{2E_0}{\pi}$$

Choice of accelerating gradient

Remarks concerning $\beta < 1$ cavities

Peak fields

The peak surface electric and magnetic fields constitute the ultimate limit for the accelerating gradient => minimize the ratio E_p/E_a and B_p/E_a .



$$E = J_0\left(\frac{2.405 \cdot r}{R}\right) \cdot E_0 e^{i\omega_0 t}$$

$$B_\varphi(r) = \frac{i}{c} J_1\left(\frac{2.405 \cdot r}{R}\right) \cdot E_0 e^{i\omega_0 t}$$

$$E_a = \frac{2E_0}{\pi}$$

$$\frac{B_p}{E_a} = \text{Max}_{r \in [0, R]} \frac{\frac{1}{c} J_1\left(\frac{2.405 \cdot r}{R}\right) \cdot E_0}{\frac{2E_0}{\pi}} = \frac{0.581865 \cdot \pi}{2 \cdot c} \approx 3.07 \left[\frac{\text{mT}}{\text{MV/m}} \right]$$

$$\frac{E_p}{E_a} = \text{Max}_{r \in [0, R]} \frac{J_0\left(\frac{2.405 \cdot r}{R}\right) \cdot E_0}{\frac{2E_0}{\pi}} = \frac{\pi}{2} \approx 1.57$$

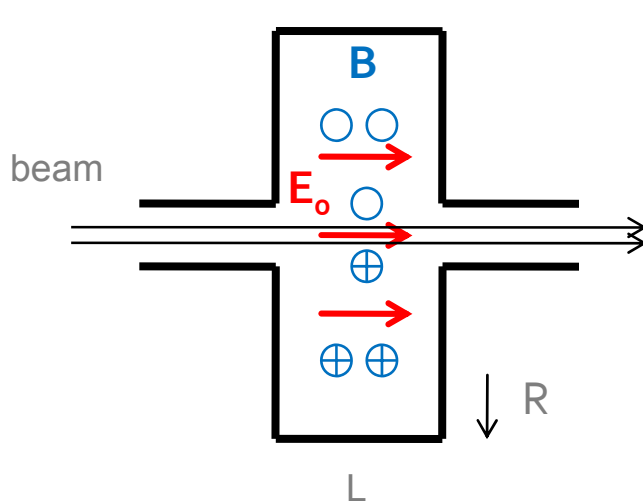
Choice of accelerating gradient
Remarks concerning $\beta < 1$ cavities

Radial field distribution of $\beta < 1$ resonator

For an accelerating cavity (π – mode, $\beta = 1$):

$$\gamma \cdot L = i\pi = i\gamma \cdot c \cdot \frac{T}{2} = i\gamma \cdot \frac{c}{2 \cdot f} = i\gamma \cdot \frac{c \cdot \pi}{2 \cdot \pi \cdot f} = i\gamma \cdot \frac{c \cdot \pi}{\omega} \Rightarrow \gamma = i \frac{\omega}{c}$$

and for $\beta < 1$): $\gamma \cdot \beta \cdot L = i\pi = \dots = i\gamma \cdot \beta \cdot \frac{c \cdot \pi}{\omega} \Rightarrow \gamma = i \frac{\omega}{\beta \cdot c}$



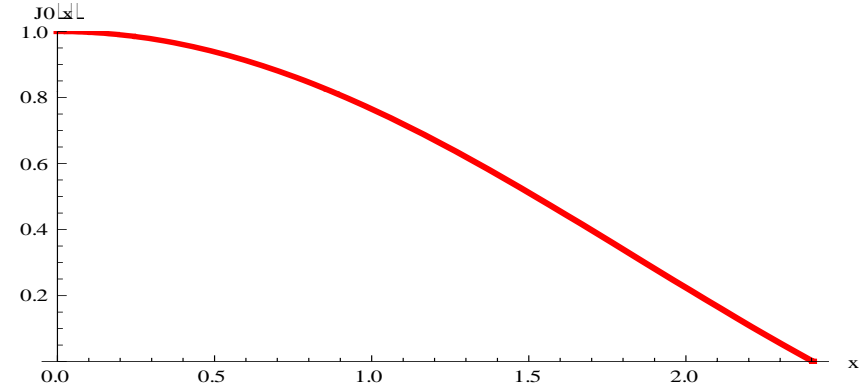
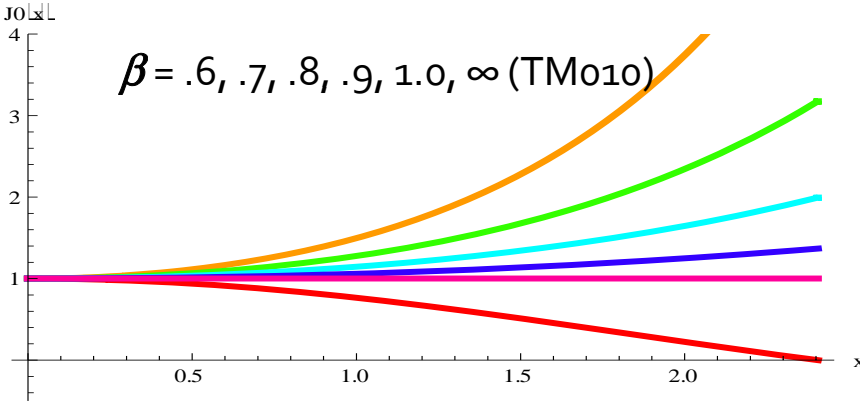
$$\nabla_{xy}^2 E_z = -(\gamma^2 + \overbrace{k^2}^{(\omega/c)^2}) E_z$$

$$\nabla_{xy}^2 E_z + \gamma^2 \left(1 + \frac{k^2}{\gamma^2}\right) E_z = \nabla_{xy}^2 E_z - \left(\frac{\omega}{c}\right)^2 \left(\frac{1}{\beta^2} - 1\right) E_z = 0$$

Choice of accelerating gradient

Remarks concerning $\beta < 1$ cavities

Comparison pillbox resonator – acc. cavity

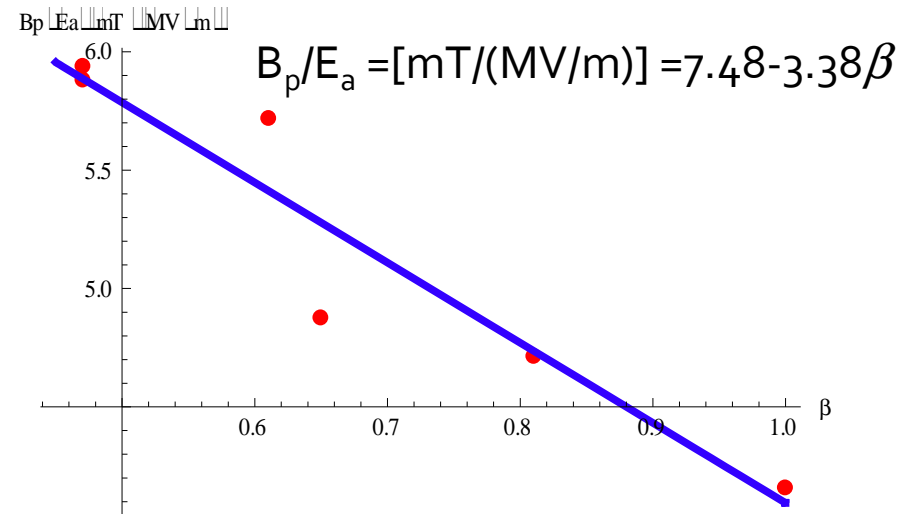
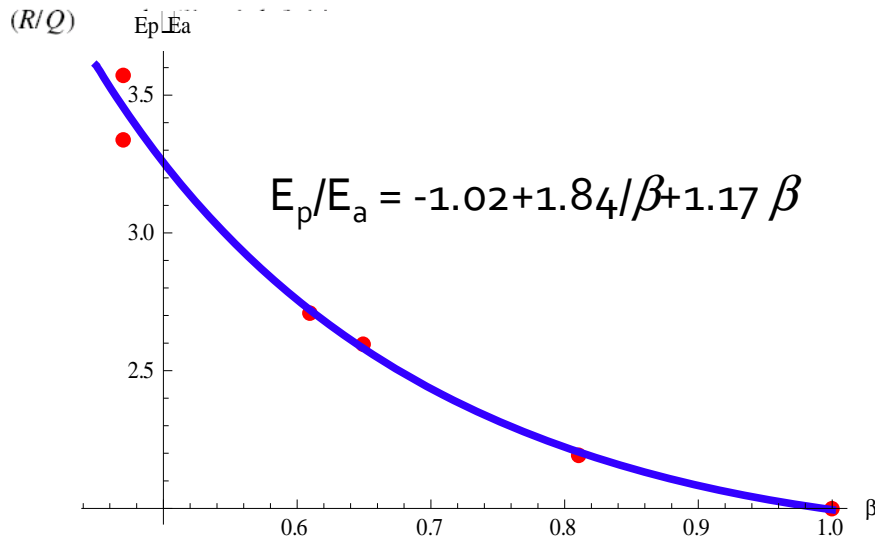
	Differential equation in the vicinity of the rotational symmetry axis Solution for fundamental transverse magnetic mode	Graph of solution
TM ₀₁₀	Bessel function J_0 $\frac{\partial^2 E_z}{\partial r^2} + \frac{1}{r} \frac{\partial E_z}{\partial r} + \left(\frac{\omega}{c}\right)^2 E_z = 0$ $E_z(r) = E_0 \cdot J_0\left(\underbrace{2.405 \cdot r/R}_x\right)$ $J_0(x) = 1 - \frac{x^2}{4} + \frac{x^4}{64} - \frac{x^6}{2304} + \dots$	
Acc. Cavity	Modified Bessel function I_0 $\frac{\partial^2 E_z}{\partial r^2} + \frac{1}{r} \frac{\partial E_z}{\partial r} + \left(\frac{\omega}{c}\right)^2 \left(1 - \frac{1}{\beta^2}\right) E_z = 0$ $E_z(r) = E_0 \cdot I_0\left(\underbrace{2.405 \cdot \sqrt{\beta^{-2} - 1} \cdot r/R}_x\right)$ $I_0(x) = 1 + \frac{x^2}{4} + \frac{x^4}{64} + \frac{x^6}{2304} + \dots$	

Choice of accelerating gradient
Remarks concerning $\beta < 1$ cavities

Technically realized peak fields for $\beta < 1$ resonator

Table 4.9: Medium- β multi-cell cavity parameters (bulk-niobium structures only)

Project	f [MHz]	β	$E_{\text{peak}}/E_{\text{acc}}$	$H_{\text{peak}}/E_{\text{acc}}$ [mT/(MV/m)]	N_{cell}	$(R/Q)/N_{\text{cell}}$ [Ω]
RIA	805	0.47	3.34	5.94	6	26.67
TRASCO	704	0.47	3.57	5.88	5	31.60
SNS medium- β	805	0.61	2.71	5.72	6	46.50
CEA/CNRS	704	0.65	2.60	4.88	5	63.00
SNS high- β	805	0.81	2.19	4.72	6	80.50
TTF	1300	1.00	2.00	4.16	9	115.11



Choice of accelerating gradient

Simulation of $Q(E_a)$

Deterministic parameters – The BCS surface resistance R_s

CW operation, using Mathematica with

- fix parameters:
 - wall thickness = 3 mm
 - Nb ($RRR = 100$)
 - geometrical length $\beta = 1$
 - residual resistance R_{res}
- with T-dependent
 - surface resistance $R_s(T_c/T)$
 - thermal conductivity λ
 - nucleate boiling heat transfer coefficient α
 - Kapitza resistance in Hell
- under the constraints of
 - max. magnetic field of $B_p = 200 \text{ mT} \cdot [1 - (T/T_c)^2]$
 - max. nucleate boiling heat flux in He of 0.5 W/cm^2
 - max. heat flux in Hell of 0.5 W/cm^2

$$R_s^{BCS} / \text{n}\Omega = 10^5 \cdot (f / \text{GHz})^2 \cdot \frac{\exp\left(-\frac{18}{T/\text{K}}\right)}{T/\text{K}}$$

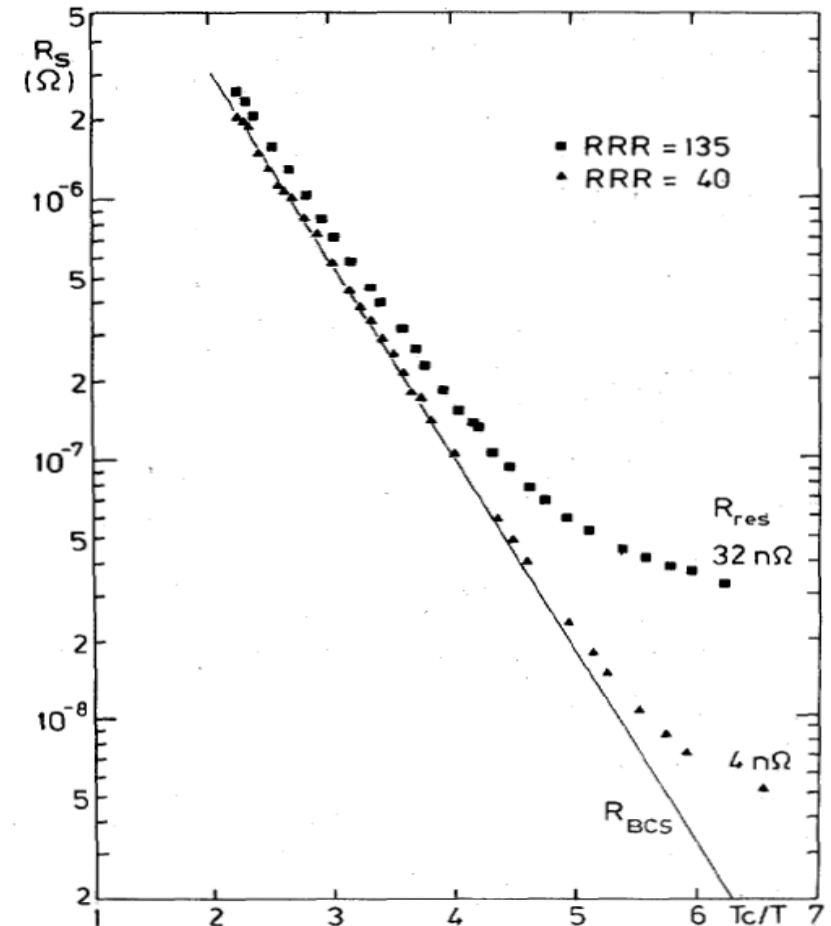


Fig. 2: Surface resistance $R_s(T)$ of two 3 GHz cavities, fabricated from niobium of different purity. $R_s(T)$ is the sum of the temperature dependent part R_{BCS} and the residual resistance R_{res} .

Choice of accelerating gradient

Deterministic parameters

Nucleate boiling heat transfer – Kapitza resistance

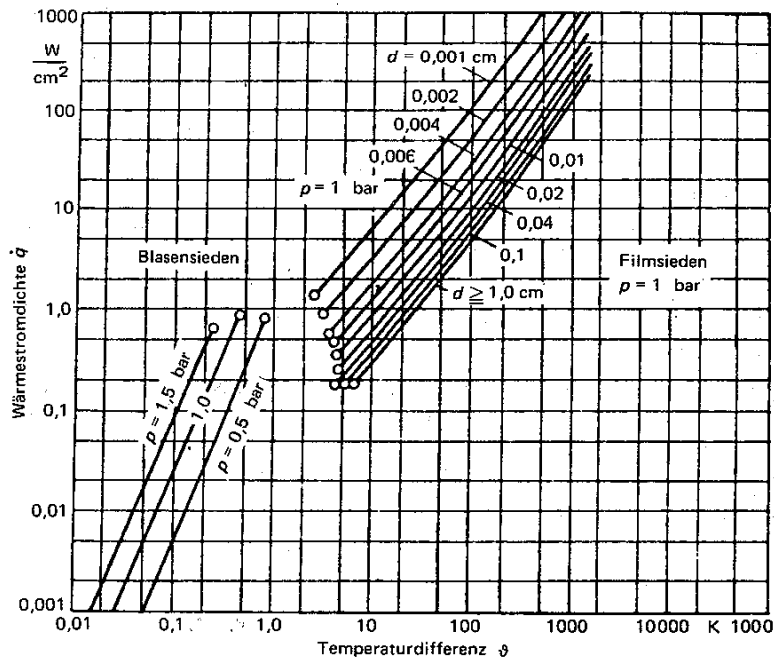
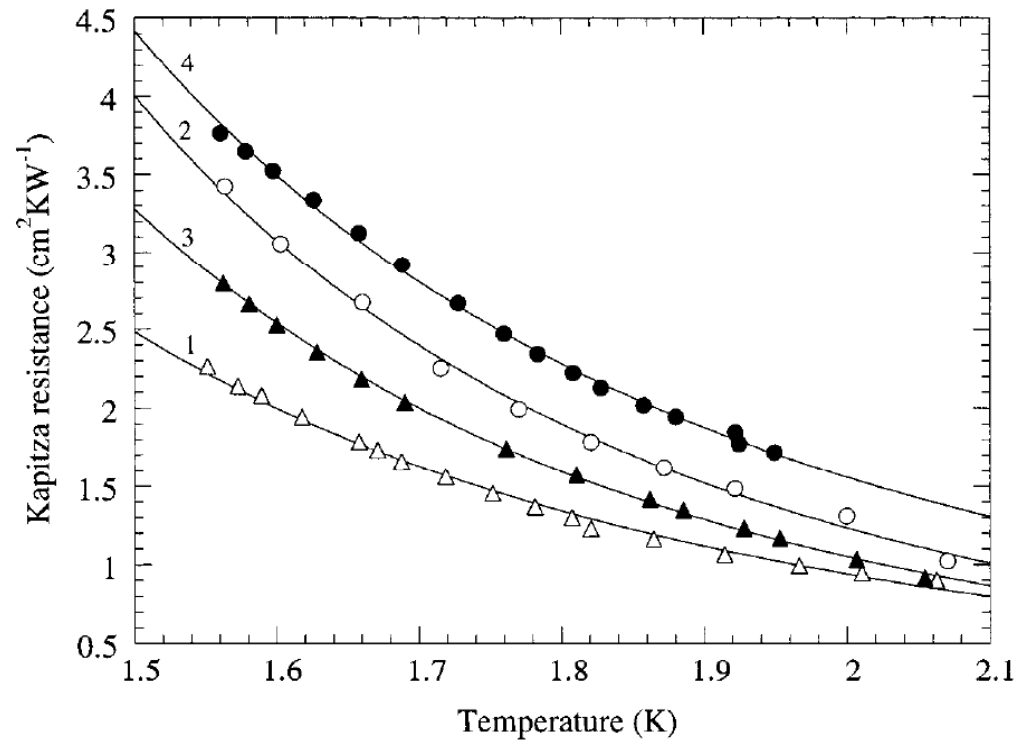


Bild 5-14. Blasen- und Filmverdampfung bei Helium.
 d Durchmesser des Heizers



H. Frey, R. A. Haefer,
Tiefemperaturtechnologie, VDI-
Verlag, Düsseldorf 1981

J. Amrit and M. X. Francois,
Journal of Low Temperature
Physics 119 (2000) 27

Choice of accelerating gradient
Deterministic parameters

Thermal conductivity

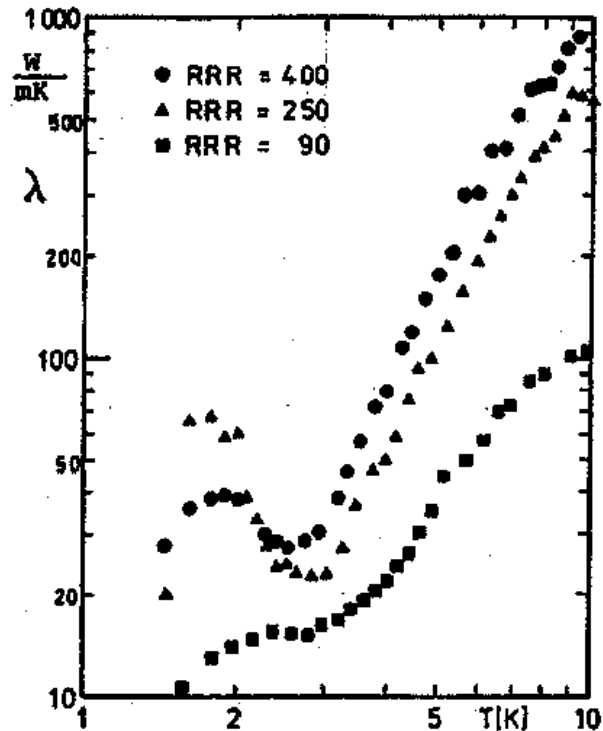


Figure 4: Thermal conductivity of Nb [4] for various purity levels. (RRR = residual resistivity ratio)

A. W. Chao, M. Tigner, Handbook of Accelerator Physics, World Scientific, Singapore 1999

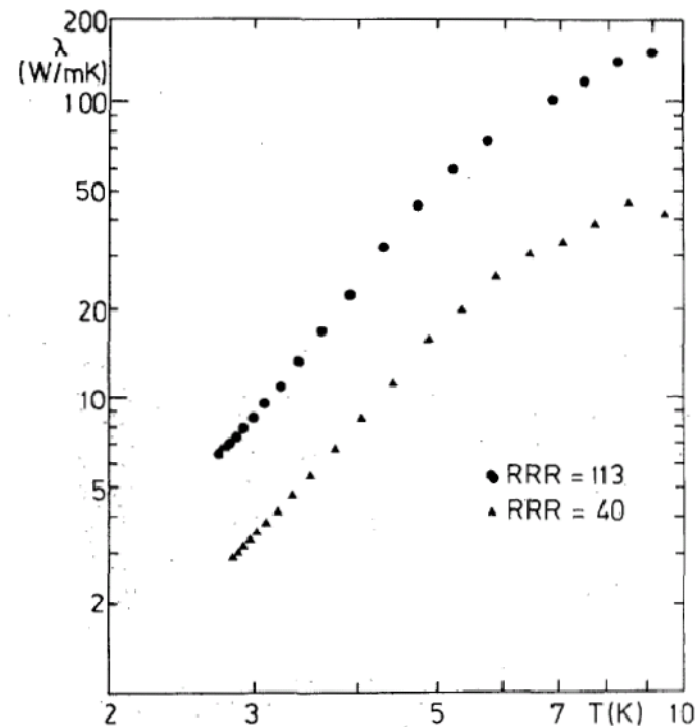


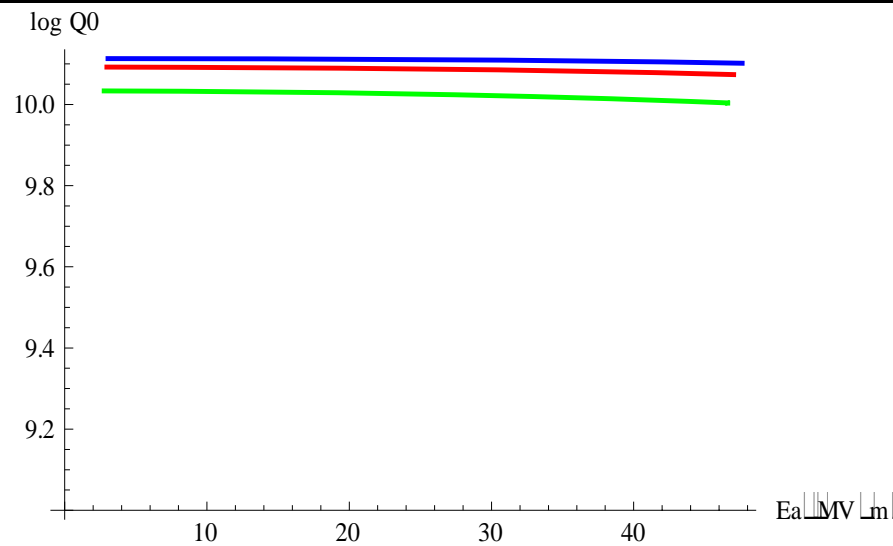
Fig. 1: Thermal conductivity of reactor grade niobium (RRR=40) and niobium of higher purity (RRR=113)

H. Lengeler, W. Weingarten, G. Müller, H. Piel, IEEE TRANSACTIONS ON MAGNETICS MAG-21 (1985) 1014

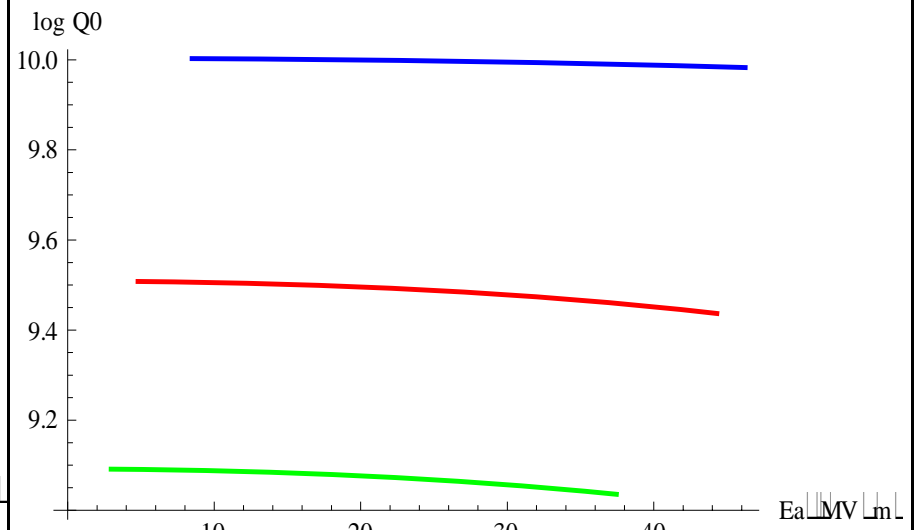
Choice of accelerating gradient
Deterministic parameters

Results of simulation : $Q(E_a)/10^9$, 704 MHz

Superfluid helium $T = 1.5, 1.8, 2.1$ K
Kapitza resistance heat transfer
RRR = 90 3 mm wall thickness



Normal helium $T = 2.2, 3.3, 4.5$ K
Nucleate boiling heat transfer
RRR = 90 3 mm wall thickness

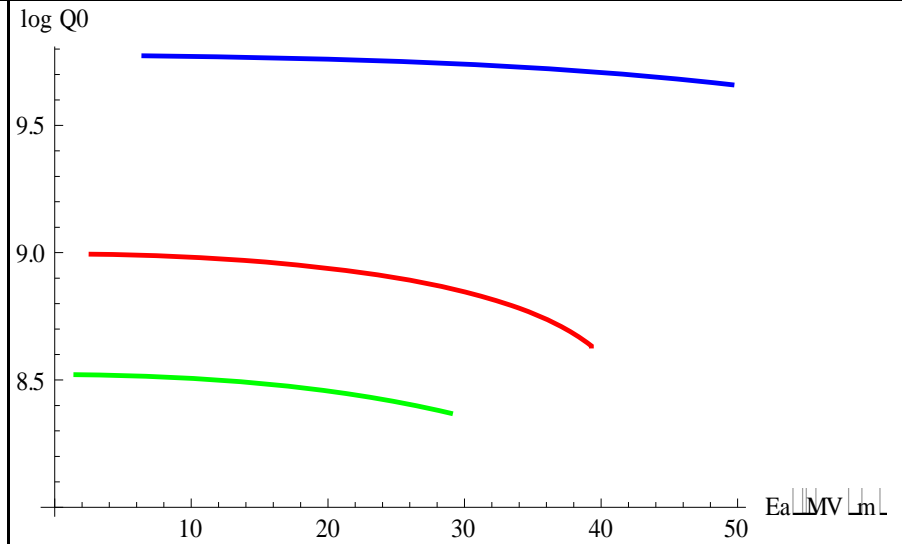
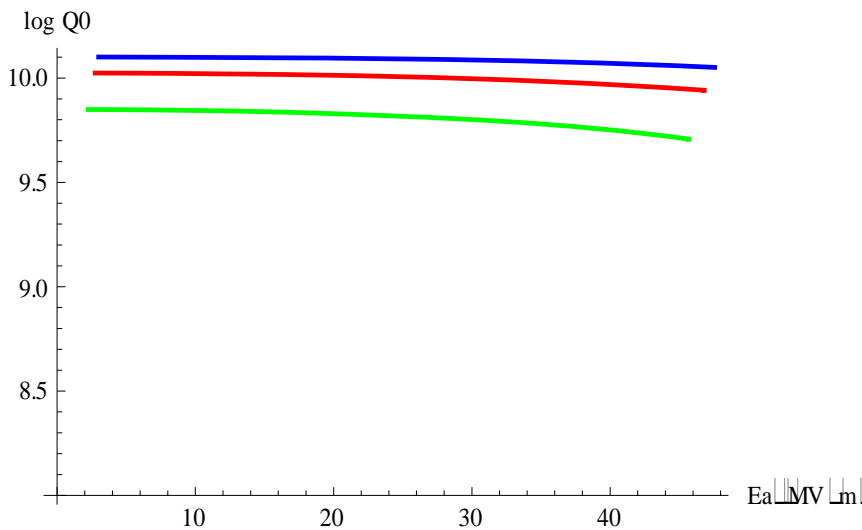


Choice of accelerating gradient
Deterministic parameters

Results of simulation : $Q(E_a) / 10^9$, 1408 MHz

Superfluid helium $T = 1.5, 1.8, 2.1$ K
Kapitza resistance heat transfer
RRR = 90 3 mm wall thickness

Normal helium $T = 2.2, 3.3, 4.5$ K
Nucleate boiling heat transfer
RRR = 90 3 mm wall thickness



Choice of accelerating gradient

Other deterministic parameters (2nd order importance)

Influencing quantity	Impact quantity	Physical explanation	Cure
External static magnetic field B_{ext}	Residual surface resistance	Creation of vortices	Shielding of ambient magnetic field by Mu-metal / Cryoperm
Residual resistivity ratio RRR	BCS surface resistance	Mean free path dependence of R_{res}	Annealing steps during ingot production/after cavity manufacture
Ratio peak magnetic field to accelerating gradient B_p/E_a	Max. accelerating gradient	Critical magnetic field as ultimate gradient limitation	Optimization of cavity shape
Nb-H precipitate	Q-value / acc. gradient (Q-disease)	Lowering of T_c/B_c at precipitates of Nb-H	T-control during chemical polishing Degassing @ 700 °C Fast cool-down

Choice of accelerating gradient

Stochastic parameters - CERN results (1985)

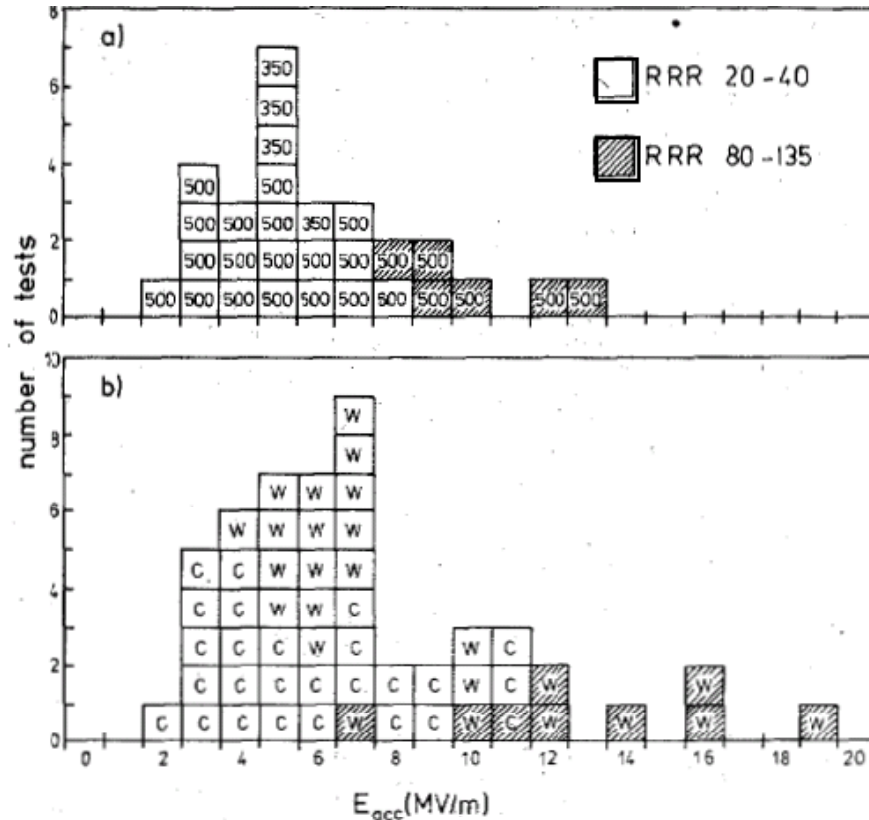


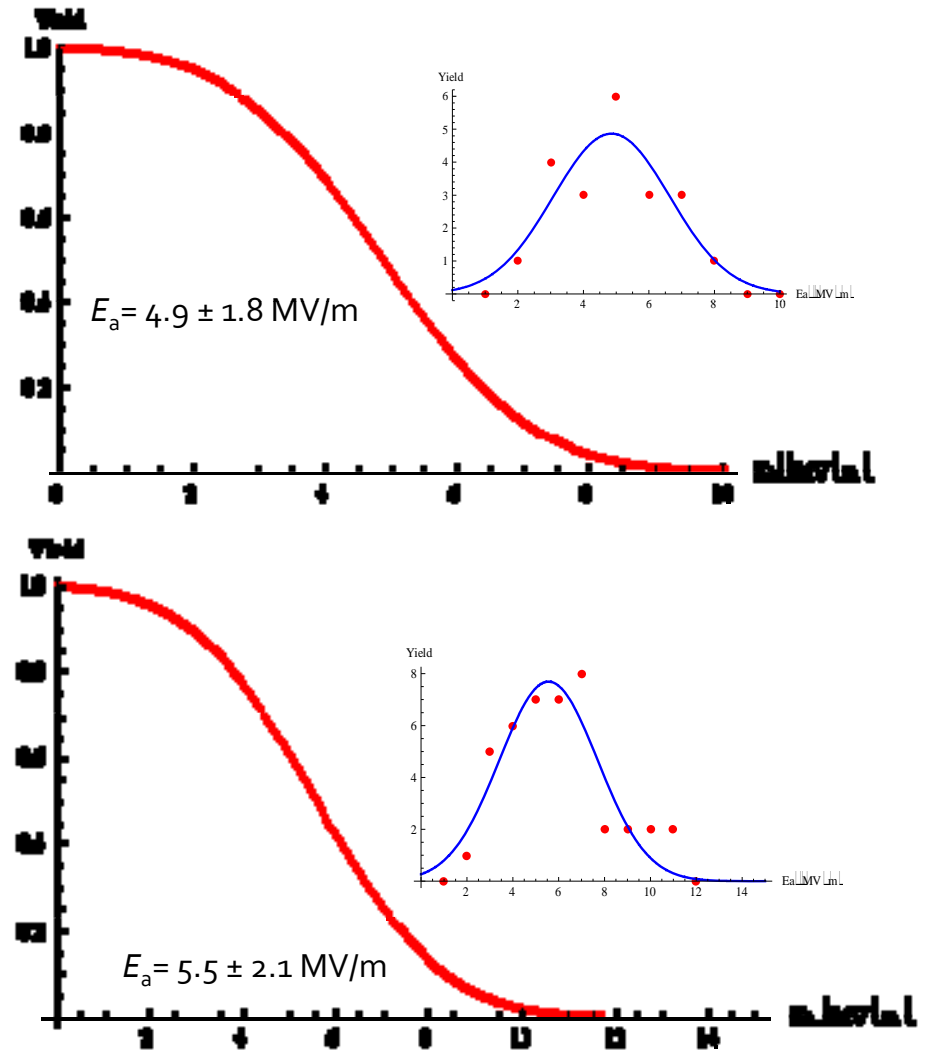
Fig. 3: Histogram of test results for single cell cavities from niobium of different RRR
 a) 500 and 350 MHz
 b) 3 GHz (CERN and Wuppertal)

H. Lengeler, W. Weingarten, G. Müller, H. Piel, IEEE
 TRANSACTIONS ON MAGNETICS MAG-21 (1985)

1014

30 April 2008

SPL Review @ CERN - WW



Choice of accelerating gradient Stochastic parameters

DESY results

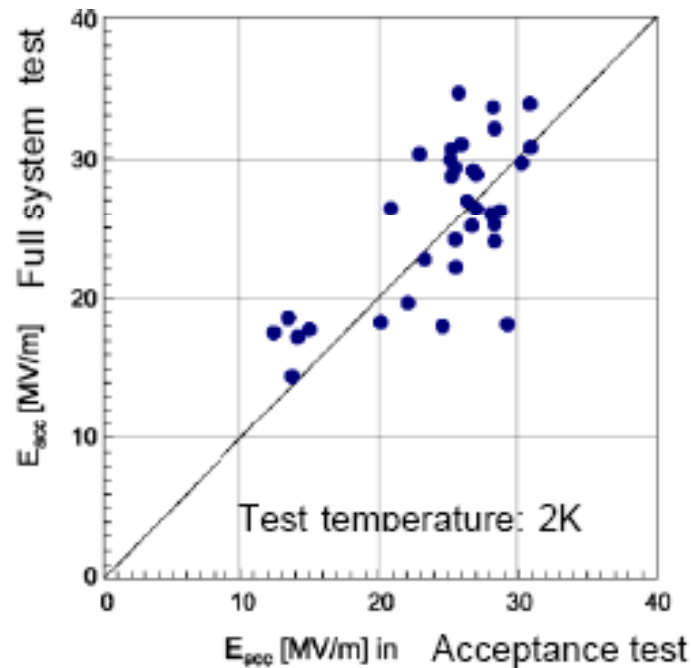


Figure 5: Comparison of cw acceptance test with full systems test (without beam)

No significant degradation of cavity performance between acceptance tests and full system tests.

Choice of accelerating gradient Stochastic parameters - DESY results

Q (Ea)

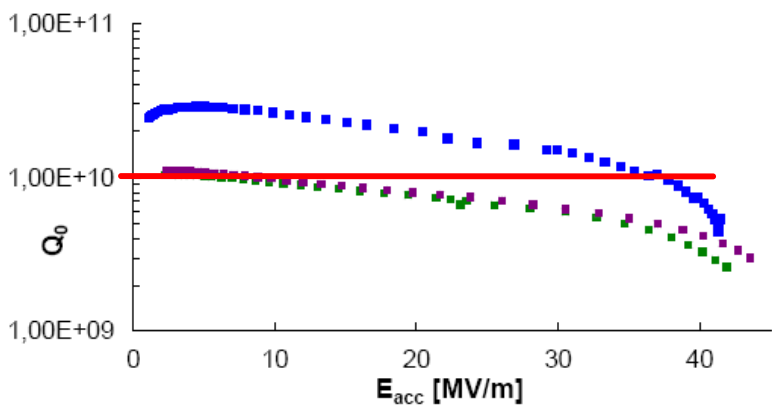


Figure 7: Example excitation curves of three welded electropolished niobium single-cell cavities. Test was done at 1.6 and 2K [9].

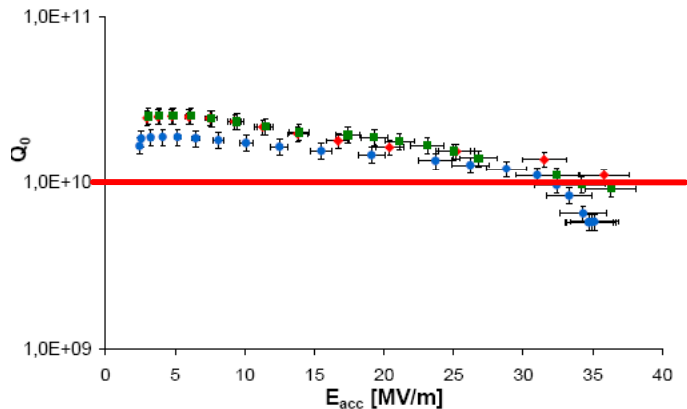


Figure 9: CW test results on three electropolished 9-cell resonators of the TESLA type from the last production series. Test was done at 2K.

A residual surface resistance corresponding to a Q-value of 10^{10} at the operating gradient presents a challenge.

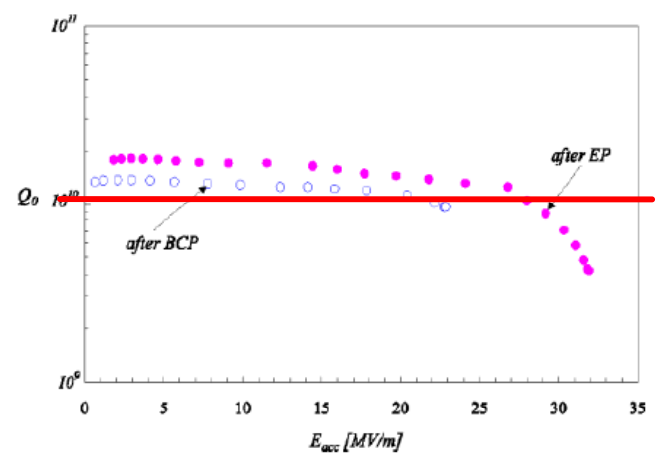


Figure 8: Result on an electropolished 9-cell cavity from the first production series. A clear improvement is seen as compared to its behavior after etching (BCP). Test was done at 2K [1].

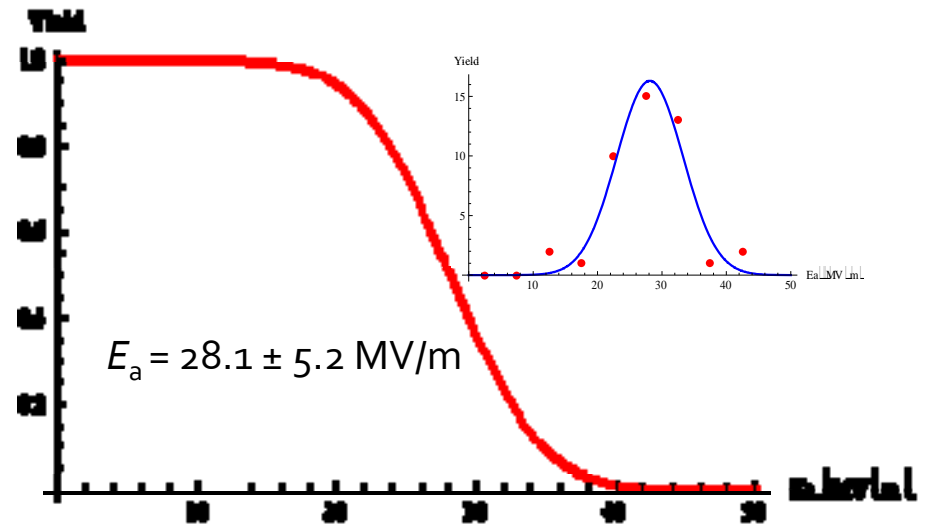
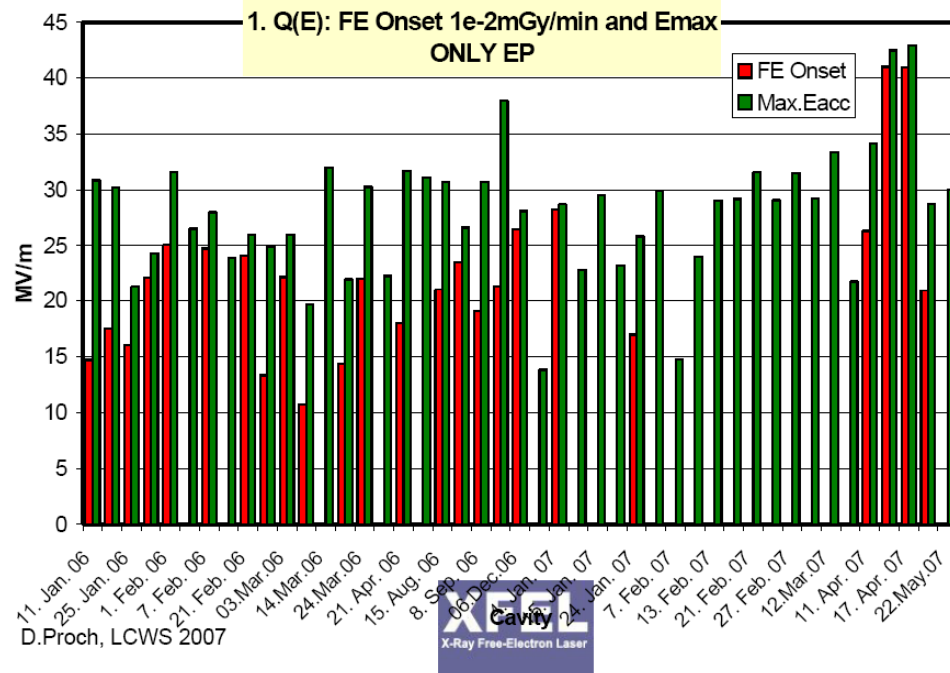
Choice of accelerating gradient Stochastic parameters - DESY results

Series tests E_a

Development of Field Emission since Jan 06

compiled by D.Reschke

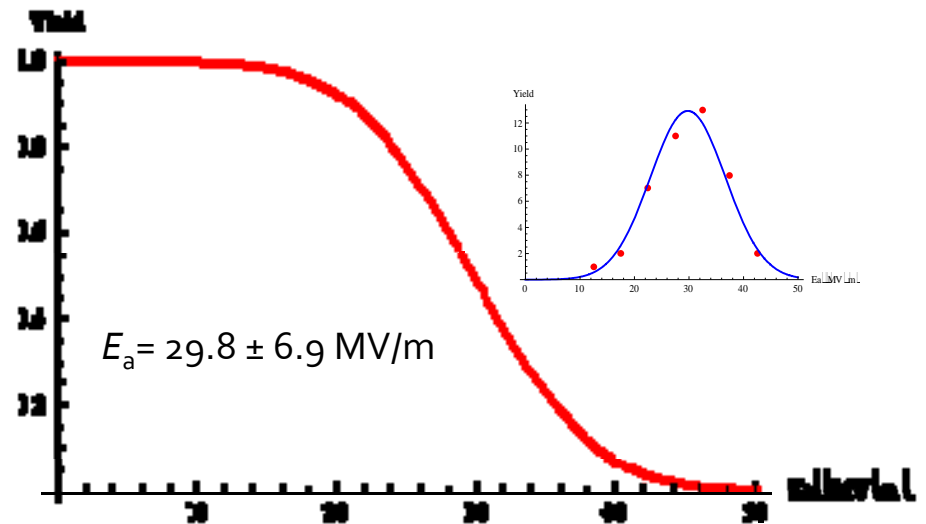
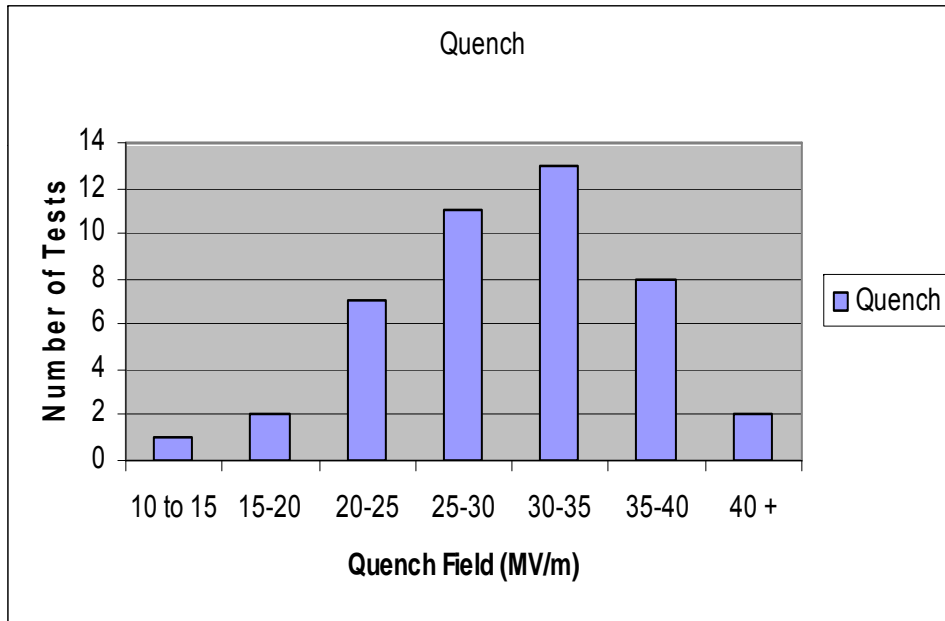
- Analysis of 1. Q(E)-results **only EP cavities** (all tests, not preparations):



Choice of accelerating gradient
Stochastic parameters - DESY results

Gradient spread Due to Quench

Probability of "Quench Only" DESY 9-cell Cavities (EP cavities only)



Compiled by H.Padamsee from DESY Data Base, TTC Meeting at DESY, January 14 - 17, 2008 <https://indico.desy.de/conferenceOtherViews.py?view=standard&confId=401>

Choice of accelerating gradient Stochastic parameters - DESY results

1 cell vs. 9 cells 1.3 GHz

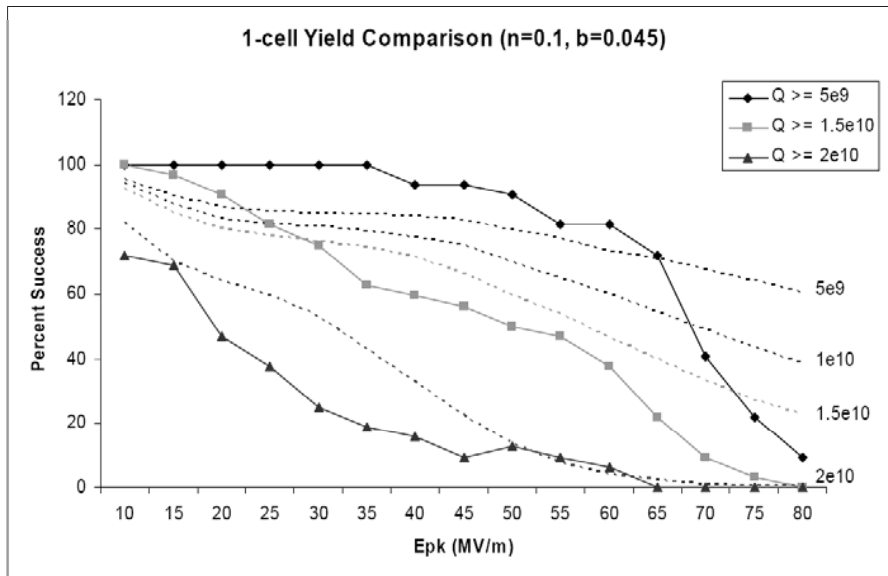


Figure 5: Simulated vs. observed yield profiles for 1-cells

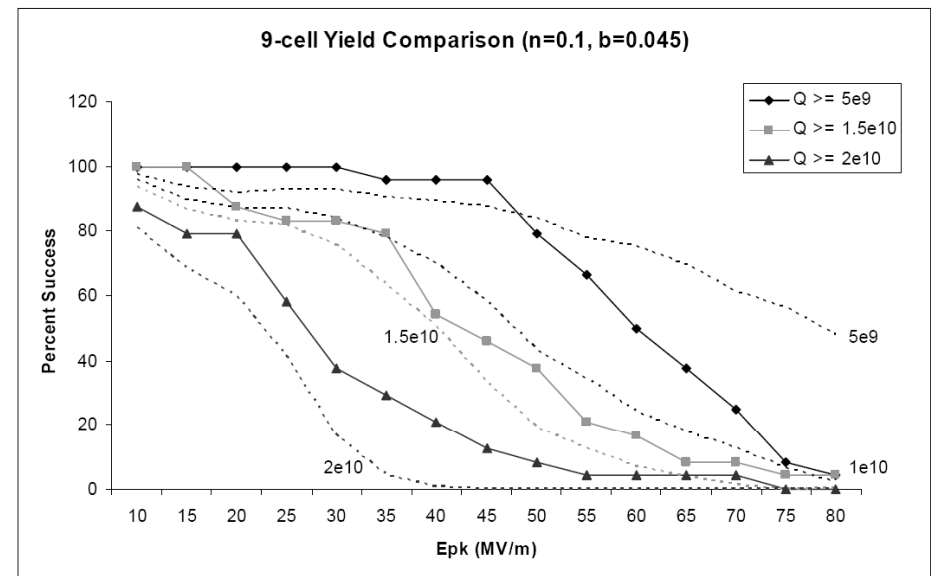


Figure 6: Simulated vs. observed yield profiles for 9-cells

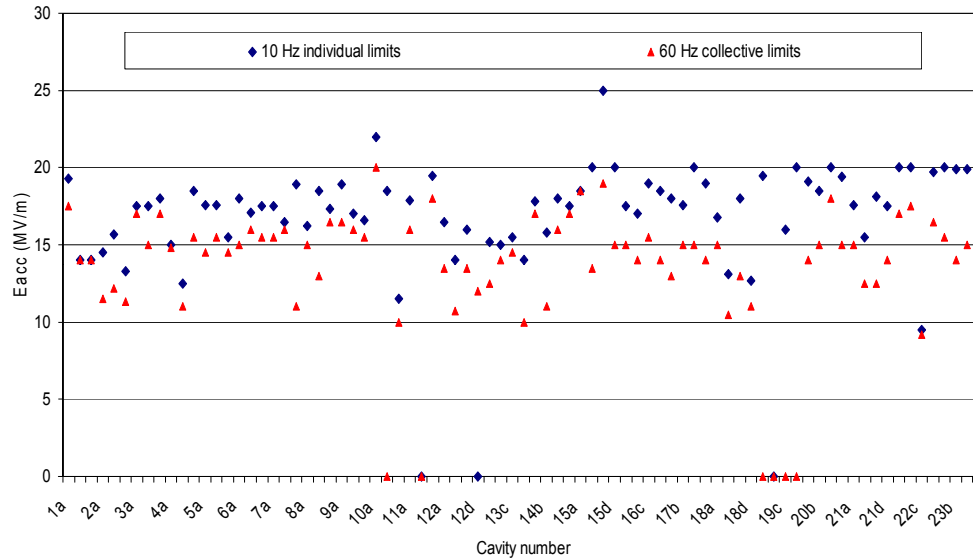
From TESLA report 2008-02
J. Wiener, H. Padamsee

On all cavities prepared by EP + low-temp baking:
1-cell or 9-cells seem not to show different results

Choice of accelerating gradient

Stochastic parameters

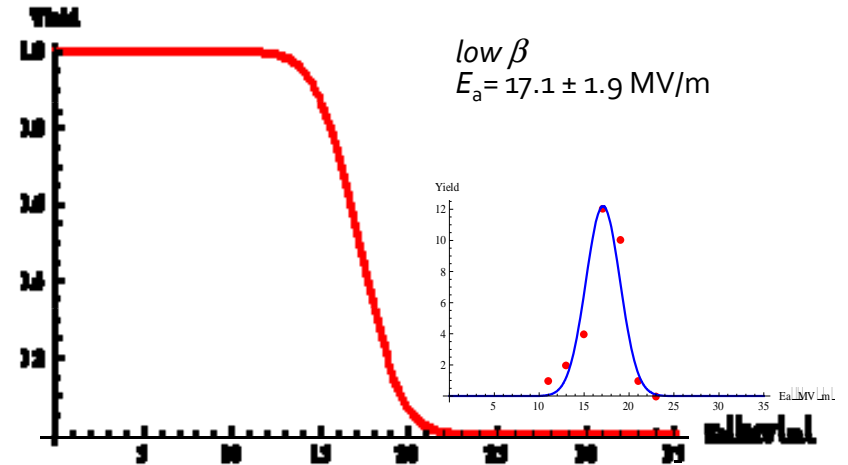
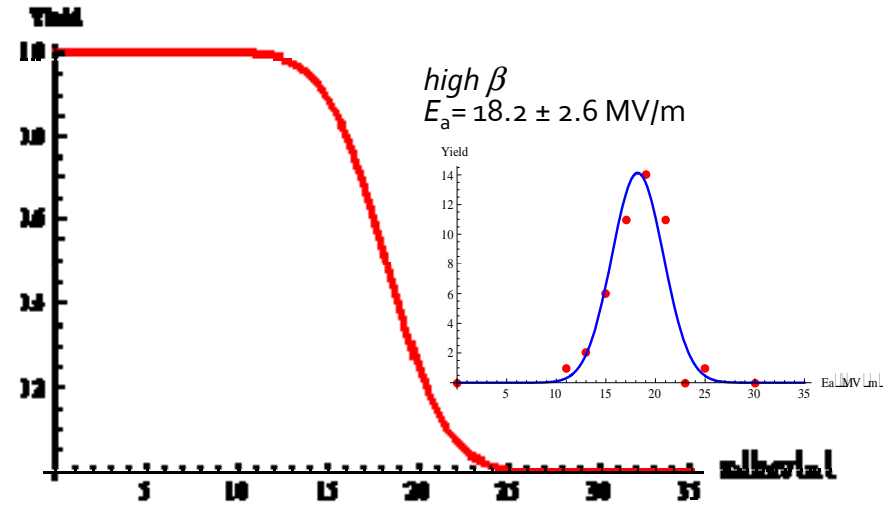
ORNL/JLAB results



Source: I. E. Campisi and S.-H. Kim, **SNS Superconducting Linac operating experience and issues**, Accelerator Physics and Technology Workshop for Project X, November 12-13, 2007
<http://projectx.fnal.gov/Workshop/Breakouts/HighEnergyLinac/agenda.html>

30 April 2008

SPL Review @ CERN - WW



Choice of accelerating gradient

Stochastic parameters

Summary of results in other labs

Laboratory	$\langle E_a \rangle$ [MV/m]	ΔE_a [MV/m]	$\Delta E_a / \langle E_a \rangle$ [%]	$\langle E_a \rangle$ [MV/m] @ 90 (50) [%] processing yield *)
CERN @ 1985 350 – 500 MHz 1-cell	4.9	1.8	37	3 (4.9)
CERN/Wuppertal @ 1985 3 GHz 1-cell	5.5	2.1	38	3 (5.5)
DESY 1.3 GHz (all)	28	5.2	19	22 (28)
ditto (quench) 9-cell	30	6.9	23	23 (30)
ORNL/JLAB SNS 805 MHz $\beta = 0.61$ 6-cell	17.1	1.9	11	15 (17)
$\beta = 1$ (extrapolated)	23.0	2.6	11	20 (23)
$\beta = 0.81$ 6-cell	18.2	2.6	14	15 (18)
$\beta = 1$ (extrapolated)	20	2.8	14	16 (20)

*) 11 (100) [%] re-processing needed (= 1/yield)

Choice of accelerating gradient

Stochastic parameters

Influencing quantity	Impact quantity	Physical explanation	Cure
Field emission sites (foreign particles sticking to the surface, size, density)	Q – value / acc. gradient γ radiation HOM coupler quench	Modified Fowler-Nordheim-theory	Electro-polishing Assembling in dust-free air Rinsing with ultrapure water (control of resistivity and particulate content of outlet water) and alcohol High pressure ultrapure water rinsing (ditto) “He- processing” Heat treatment @ 800 – 1400 °C
Secondary emission coefficient δ	Electron-multipacting	Theory of secondary electron emission	Rounded shape of cavity Rinsing with ultrapure water Bake-out RF - Processing
<i>Unknown</i>	Q – slope / Q-drop (Q – value / acc. gradient)	<i>Unknown</i>	Annealing 150 °C Electro-polishing
Metallic normal-conducting inclusions in Nb	Acc. gradient	Local heating up till critical temperature of Nb	Inspection of Nb sheets (eddy current or SQUID scanning) Removal of defects ($\approx 1 \mu\text{m}$) Sufficiently large thermal conductivity (30 - 40 [W/(mK)])
Residual surface resistance	Q – value / acc. gradient	<i>Unknown to large extent</i>	Quality assurance control of a multitude of parameters

Choice of operating temperature and frequency

Power grid – beam transfer efficiency (T_b, ω)

Simulation parameters

High Power SPL

$\beta = 1$
 $E_a = 25$ MV/m
 $R_{\text{res}} = 24$ n Ω
 $n = 5$
 $\tau = 0.72$ msec
 $I_b = 40$ mA
 $T_{\text{in}} = 0.64$ GeV
 $T_{\text{out}} = 5$ GeV
 $\phi = 20$ degrees
 $r = 50$ sec⁻¹
 $\eta_{\text{real-estate}} = 0.5$
 $\eta_{\text{Rf}} = 0.4$
 $\eta_{\text{td}} = 0.2$
 $P_{\text{cst}} = 15$ W/m

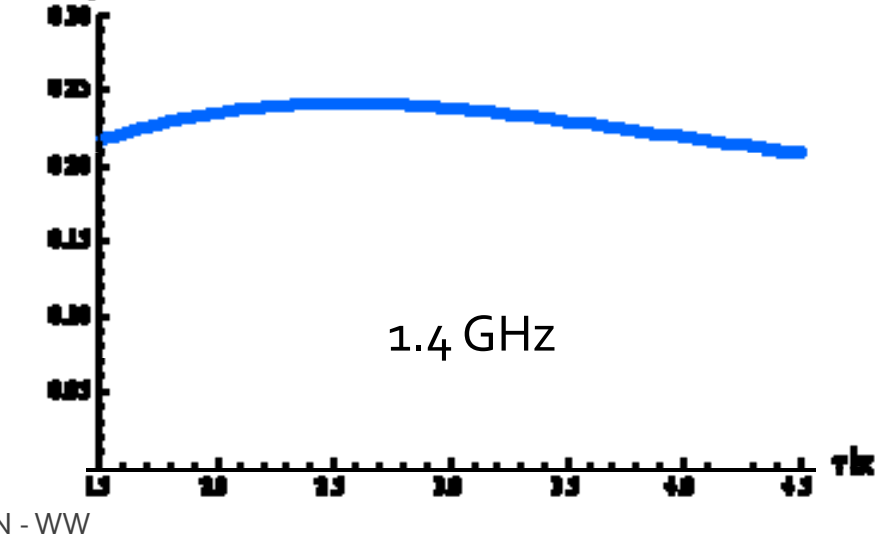
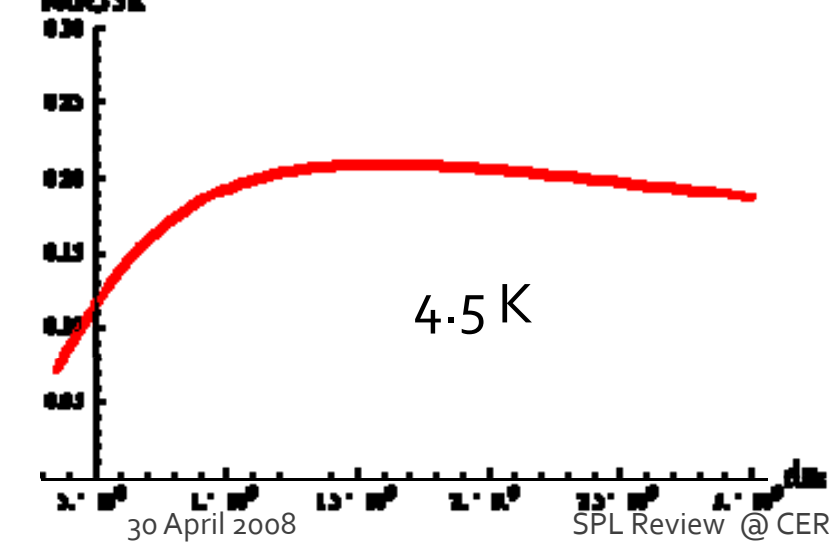
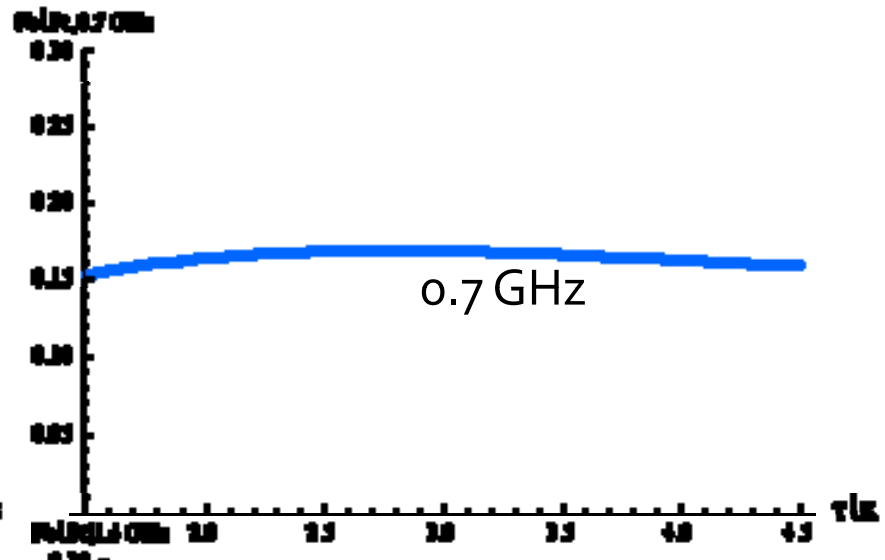
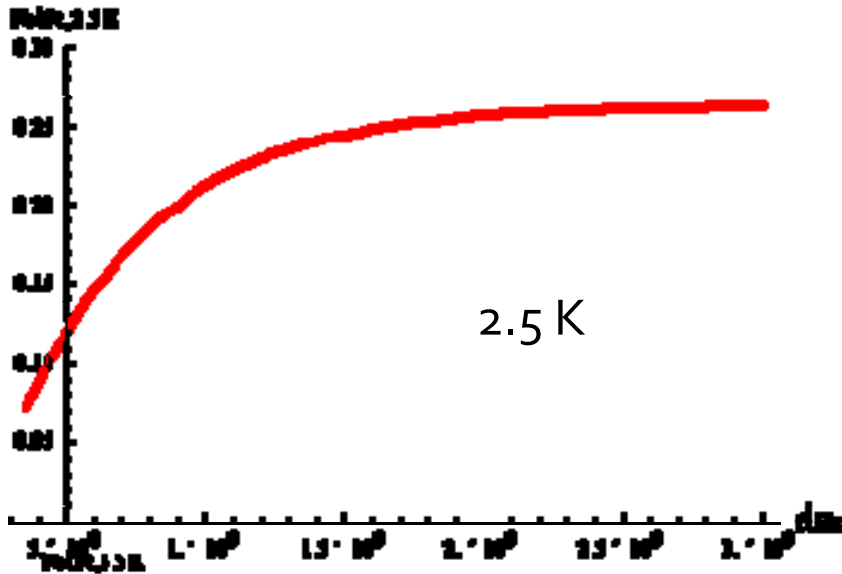
Low Power SPL

$\beta = 1$
 $E_a = 25$ MV/m
 $R_{\text{res}} = 24$ n Ω
 $n = 5$
 $\tau = 1.2$ msec
 $I_b = 20$ mA
 $T_{\text{in}} = 0.64$ GeV
 $T_{\text{out}} = 4$ GeV
 $\phi = 20$ degrees
 $r = 2$ sec⁻¹
 $\eta_{\text{real-estate}} = 0.5$
 $\eta_{\text{Rf}} = 0.4$
 $\eta_{\text{td}} = 0.2$
 $P_{\text{cst}} = 15$ W/m

Choice of operating temperature and frequency

Power grid – beam transfer efficiency (T_b, ω)

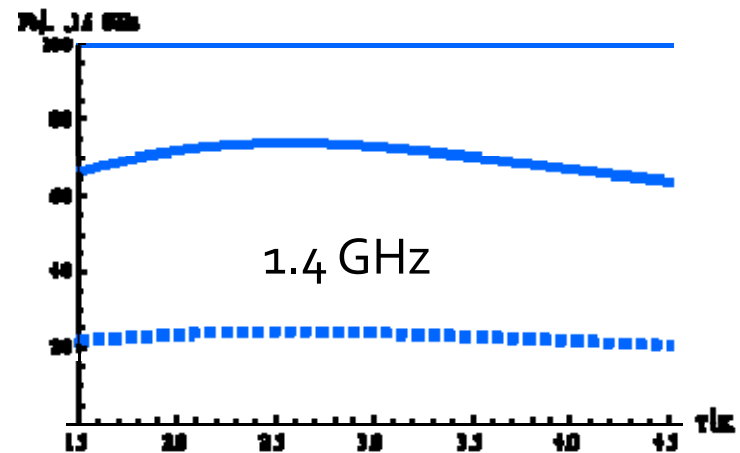
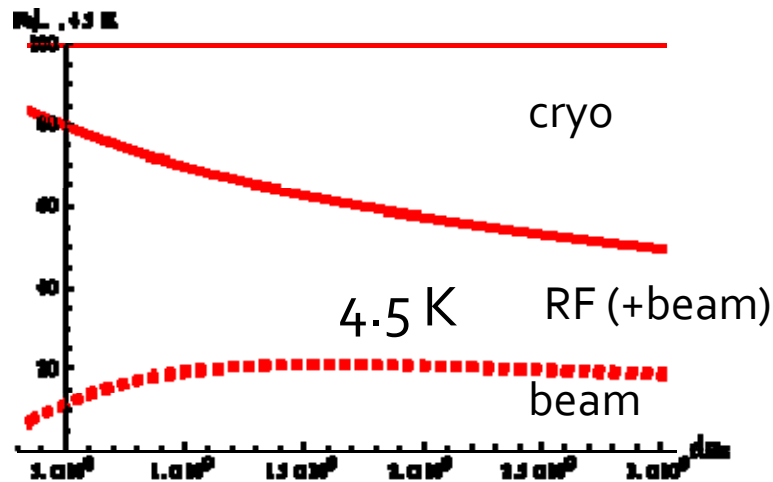
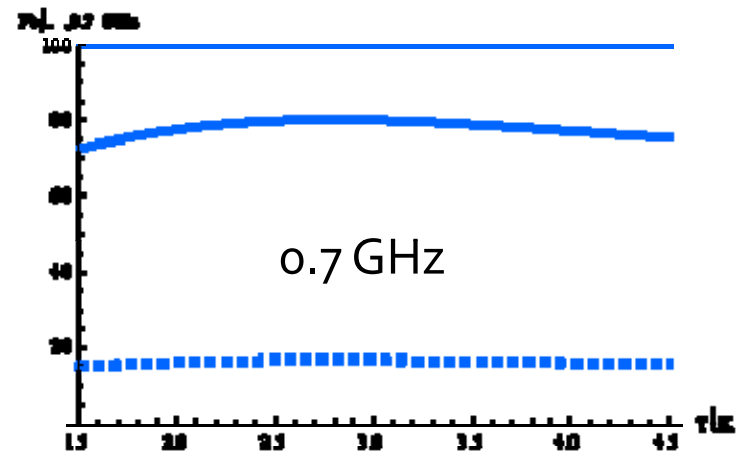
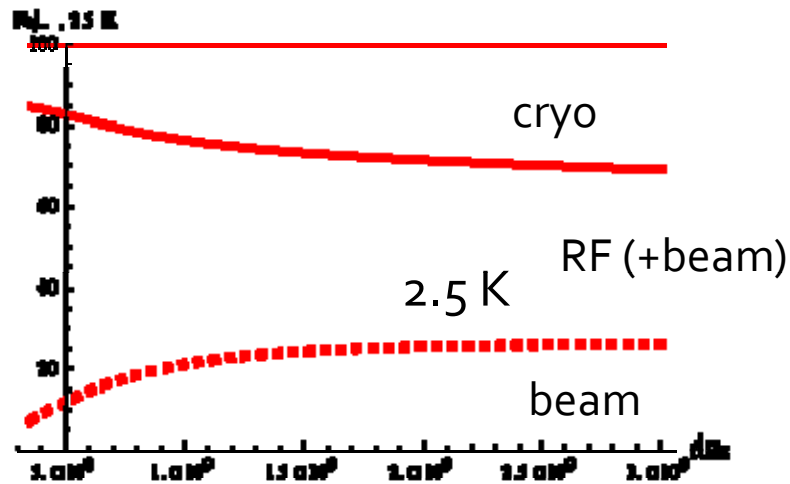
Results high power SPL



Choice of operating temperature and frequency

Results high power SPL

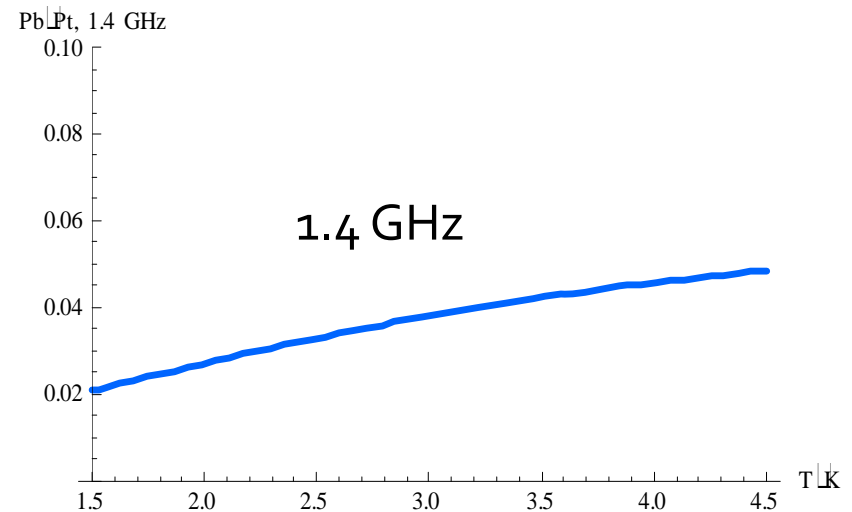
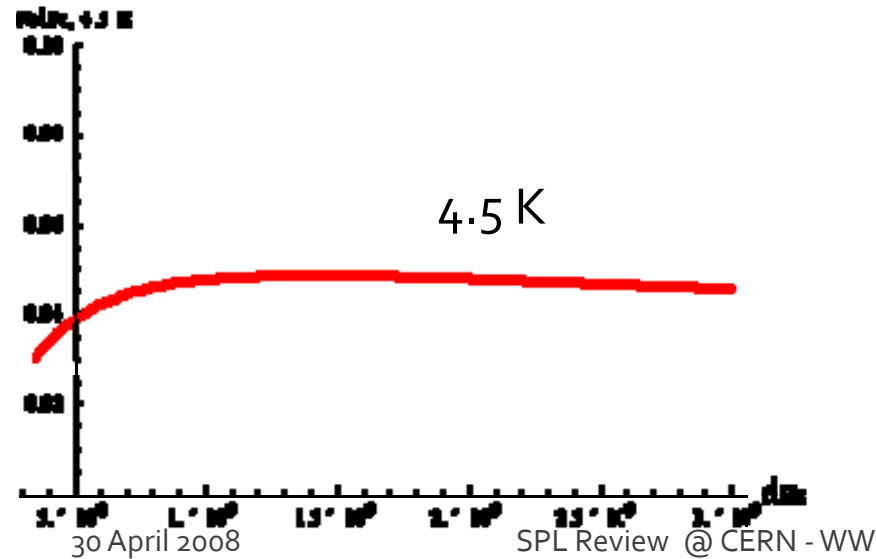
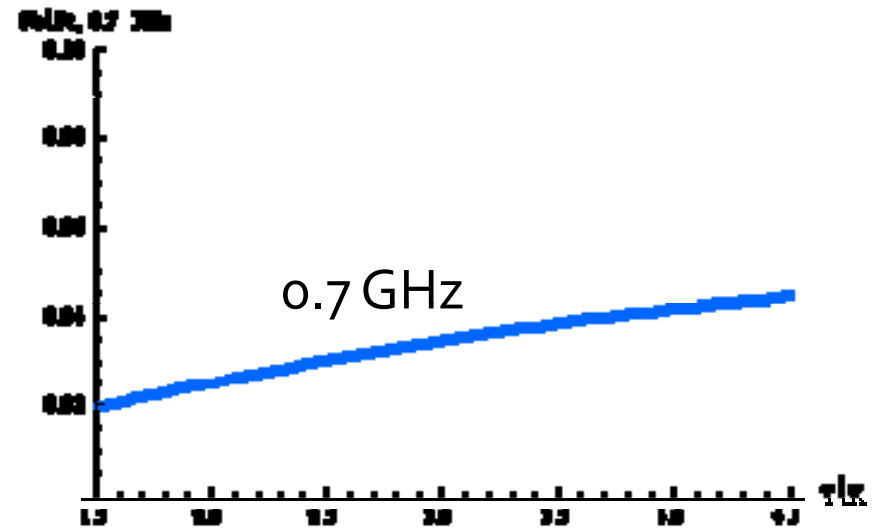
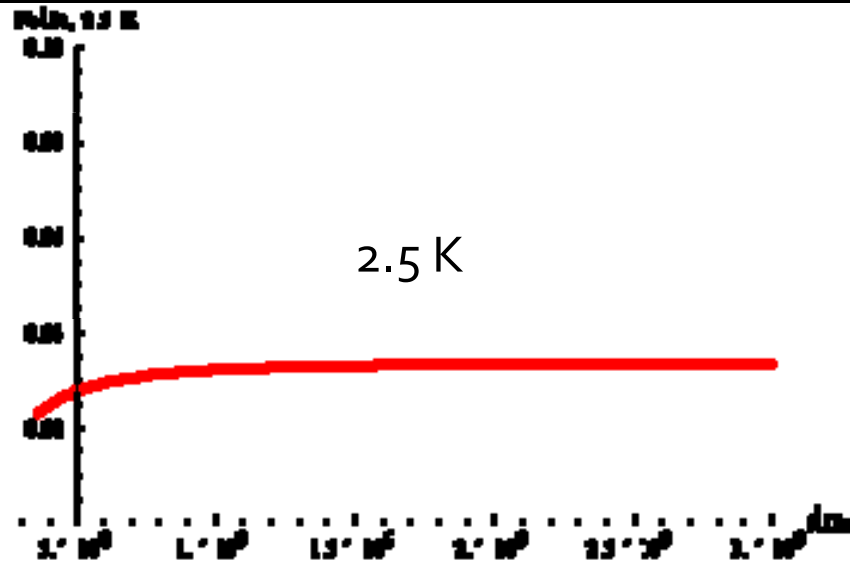
Total power sharing [%]



Choice of operating temperature and frequency

Power grid – beam transfer efficiency (T_b, ω)

Results low power SPL



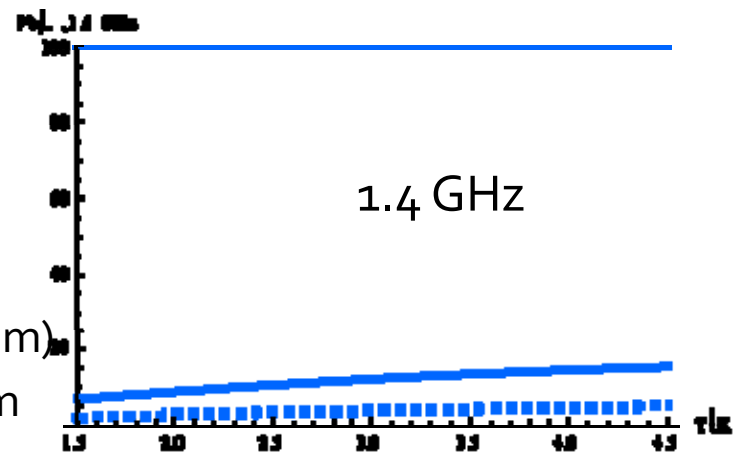
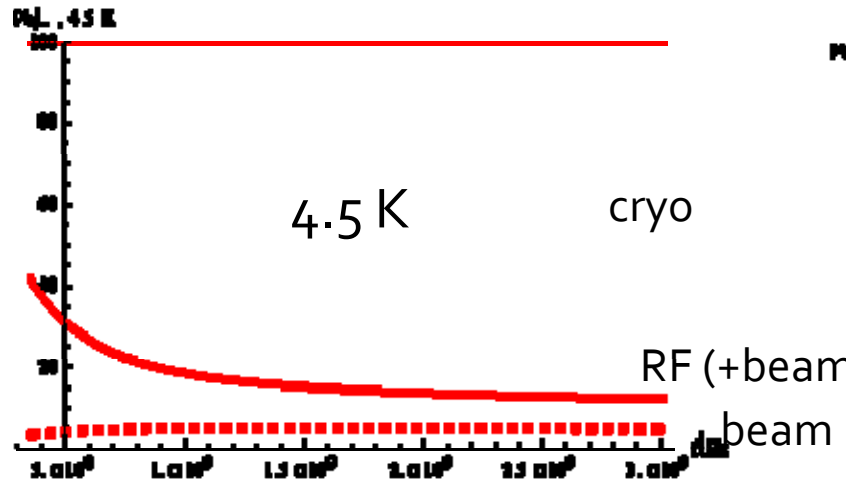
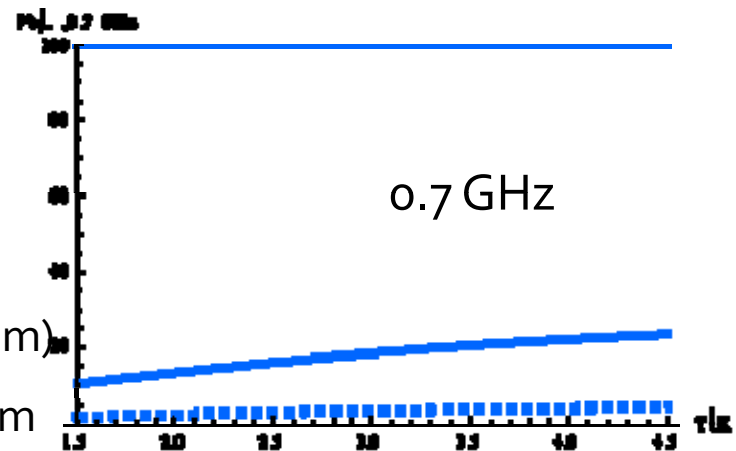
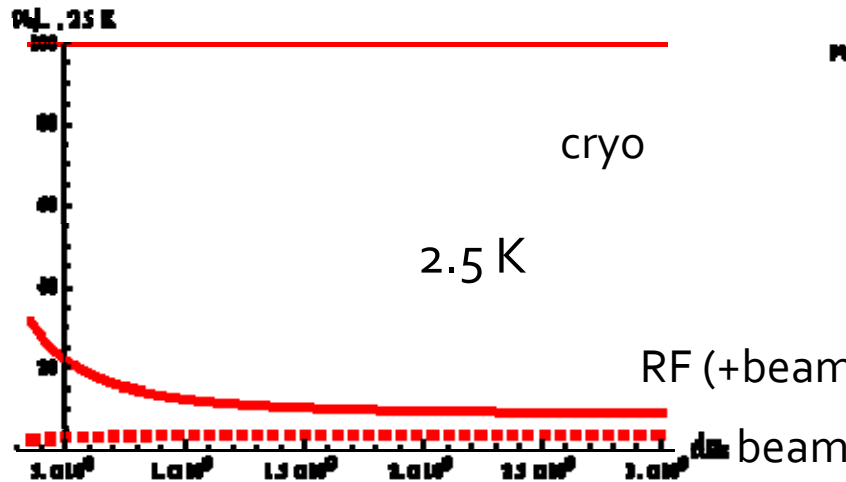
30 April 2008

SPL Review @ CERN - WW

Choice of operating temperature and frequency

Results low power SPL

Total power sharing [%]



Choice of operating temperature and frequency

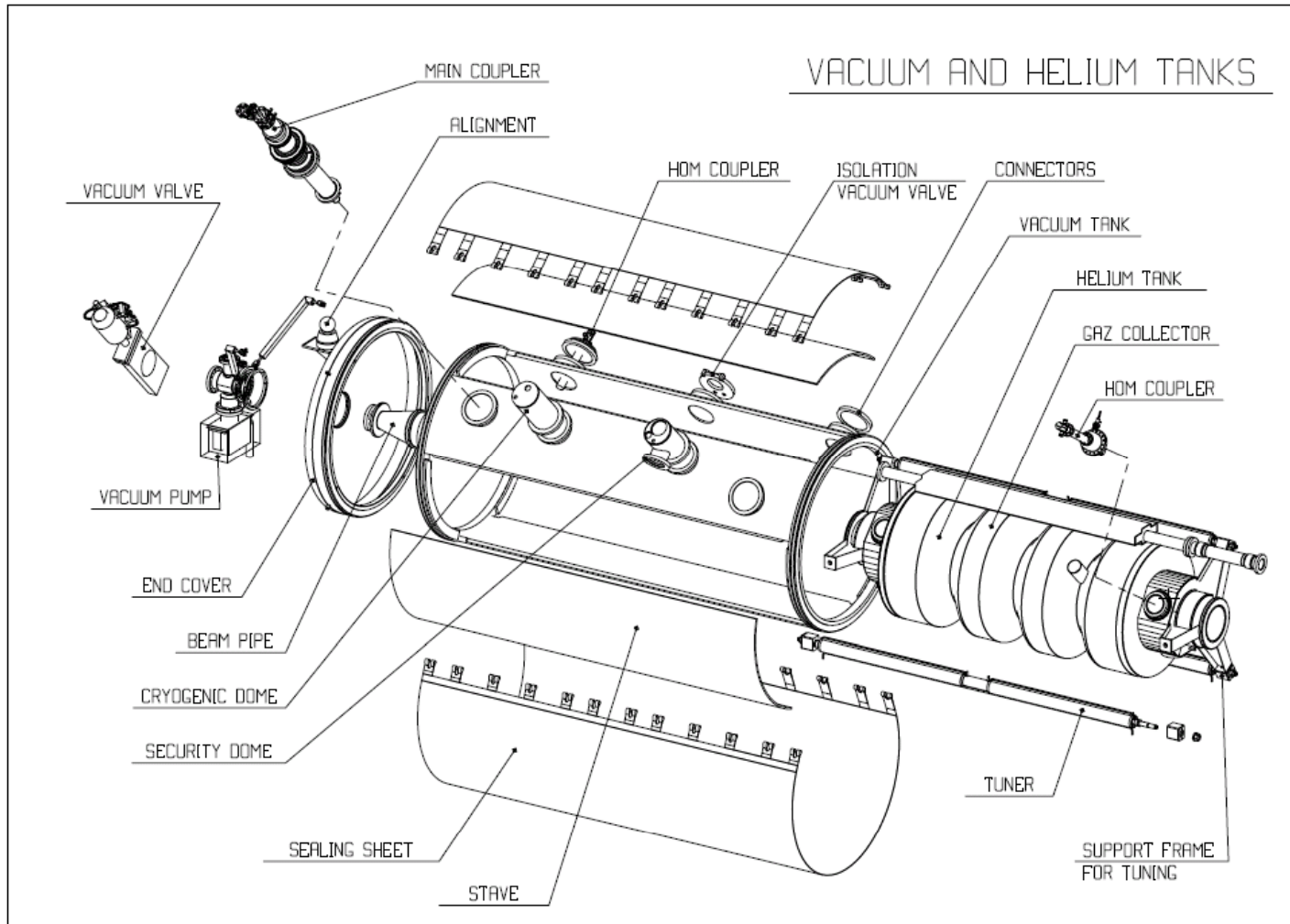
Remarks concerning cryostat

Comparison of planned and existing sc linacs

	(LEP)	LP-SPL high β	HP-SPL high β	SNS high β	Project X	XFEL	ILC
f [MHz]	352	704	704	805	1300	1300	1300
Beam energy on target [GeV]	100	4	5	1	8	20	500
Beam current in bunch train [mA]	3	20	40	26	9	5	9
Pulse duty factor [%]	100	0.2	2.0	6.0	0.5	0.7	0.5
Acc. gradient E_a = voltage gain / active length [MV/m]	6	25	25	18	32	24	31.5
E_p/E_a	2.3	2.0	2.0	2.1	2.0	2.0	2
B_p/E_a [mT/MV/m]	3.9	4.0	4.0	4.6	4.3	4.3	4.3
Operating temperature [K]	4.5	2.0	2.0	2.1	2.0	2.0	2.0
Unloaded Q-factor [10^{10}] @ nominal gradient	0.32	1	1	0.5	1	1	1
Dissipated power per cavity at nominal gradient [W]	70	0.3	2.5	6.1	0.5	0.4	0.5
Active length of cavity [m]	1.7	1.07	1.07	0.91	1.04	1.04	1.04
Max. power per cavity [MW]	0.06	0.5	1.1	0.4	0.3	0.1	0.3
Bunch repetition spectrum [MHz]	0.044	352	352	403	323	5	3
Number of cells per cavity	4	5	5	6	9	9	9

Choice of operating temperature and frequency

Remarks concerning cryostat



Comments:

The LEP cryostat could reliably be operated under CW conditions with beam and in pulsed conditions without beam in the present LHC tunnel environment (1.4 % slope).

It is worth noting that the He tank, the gas openings, and gHe collector were relatively small.

Pulsed operation: The thermal diffusivity $\kappa \approx \lambda / (c \cdot \rho)$ is such that it takes ~ 1 ms before the temperature pulse arrives at the niobium helium interface => advantage compared to CW operation.

This cryostat was tested under pulsed conditions with beam in the CERN SPS.

Concluding remarks

- $\beta < 1$ cavities are inherently lower in gradient, compared to $\beta = 1$ cavities, because of
 - larger radial field increase
 - lower acceleration efficiency (transit time factor).If corrected for these two effects, performances are similar.
- **Simulation of Q(Ea)** by taking into account the deterministic performance parameters -
 - such as critical magnetic fields and heat transport through niobium wall and across Nb-He interface -predicts possible operation at acc. gradients of **25 MV/m** and more at all lHe temperatures, with a smaller margin at 1408 MHz and 4.5 K.
- A residual surface resistance corresponding to a **Q-value of 10^{10}** at the operating gradient presents a challenge (because of lacking knowledge of the causes).
- Test results from **outside labs** show that acc. gradients of **16 – 23 MV/m** ($\beta = 1$ cavities) for a **production yield of 90 %** are possible.
 - Higher gradients (**20 – 30 MV/m**) are possible at the expense of a **lower production yield (~ 50%)**.
 - Electro-polished and baked 1.3 GHz **mono-cell and 9-cell** cavities exhibit no significant difference in yield.
- The power consumption for the **high power SPL** is dominated by RF. It has the largest grid to beam power transfer efficiency (~ 24 %) at **2.5 K and 1.4 GHz**.
- The power consumption for the **low power SPL** is dominated by cryogenics. The grid to beam power transfer efficiency depends only weakly on the frequency and increases with temperature (2 – 4 %).
- **Power dissipation per cavity** in the SPL in pulsed operation is by **1 – 2 orders of magnitude smaller than for the LEP cavities** in CW operation. Therefore, design considerations for the LEP cryostat could provide valuable guidelines in addition to other designs.
 - The temperature increase at the Nb-He interface is significantly reduced compared to CW for **pulsed operation** (< 1 msec pulse length).